

Supplementary Information for

Robust staggered band alignment in one- dimensional van der Waals heterostructures: binary compound nanoribbons in nanotubes

Ming Gong,[†] Guang-Ping Zhang,[§] Hui Hui Hu,[†] Liangzhi Kou,[‡] Kun Peng Dou,^{*,†} and Xing-
Qiang Shi^{*,‡}

[†]College of Information Science and Engineering, Ocean University of China, Qingdao 266100,
China

[‡]Department of Physics, Southern University of Science and Technology, Shenzhen 518055,
China *Email - shixq@sustc.edu.cn

[§]Shandong Province Key Laboratory of Medical Physics and Image Processing Technology,
School of Physics and Electronics, Shandong Normal University, Jinan 250358, China

[‡]School of Chemistry, Physics and Mechanical Engineering, Queensland University of
Technology, Gardens Point Campus, Brisbane, Queensland 4001, Australia

Table S1 Test calculations of valence band offset (VBO), conduction band offset (CBO) and band gap of BN (11,11)+Z₄ and (19,0)+A₇. Heyd–Scuseria–Ernzerhof (HSE06) hybrid functional with 25% Hartree–Fock exchange energy is employed for accurate band structure calculations.

	(11,11)+Z ₄					(19,0)+A ₇			
Energy	420	420	500	600	700	420	500	600	700
Cutoff (eV)	(PBE)	(HSE06)	(PBE)	(PBE)	(PBE)	(PBE)	(PBE)	(PBE)	(PBE)
Band gap (eV)	4.0000	5.4163	4.0000	4.0000	4.0000	4.3537	4.3536	4.3537	4.3538
CBO (eV)	0.3454	0.3785	0.3451	0.3453	0.3452	0.1739	0.1740	0.1738	0.1736
VBO (eV)	0.2285	0.4033	0.2287	0.2287	0.2288	0.2255	0.2250	0.2249	0.2250

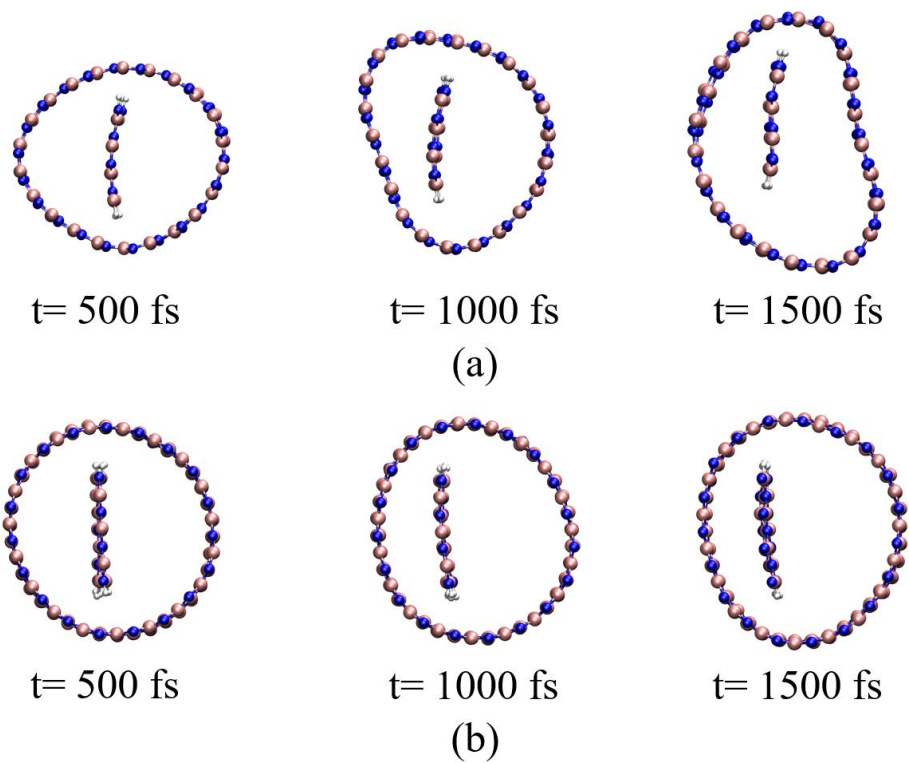


Figure S1 Snapshots of AIMD simulation for (a) (11,11)+Z₄ and (b) (19,0)+A₇ at a temperature of 300 K. Both composites remain stable over 1500 fs.

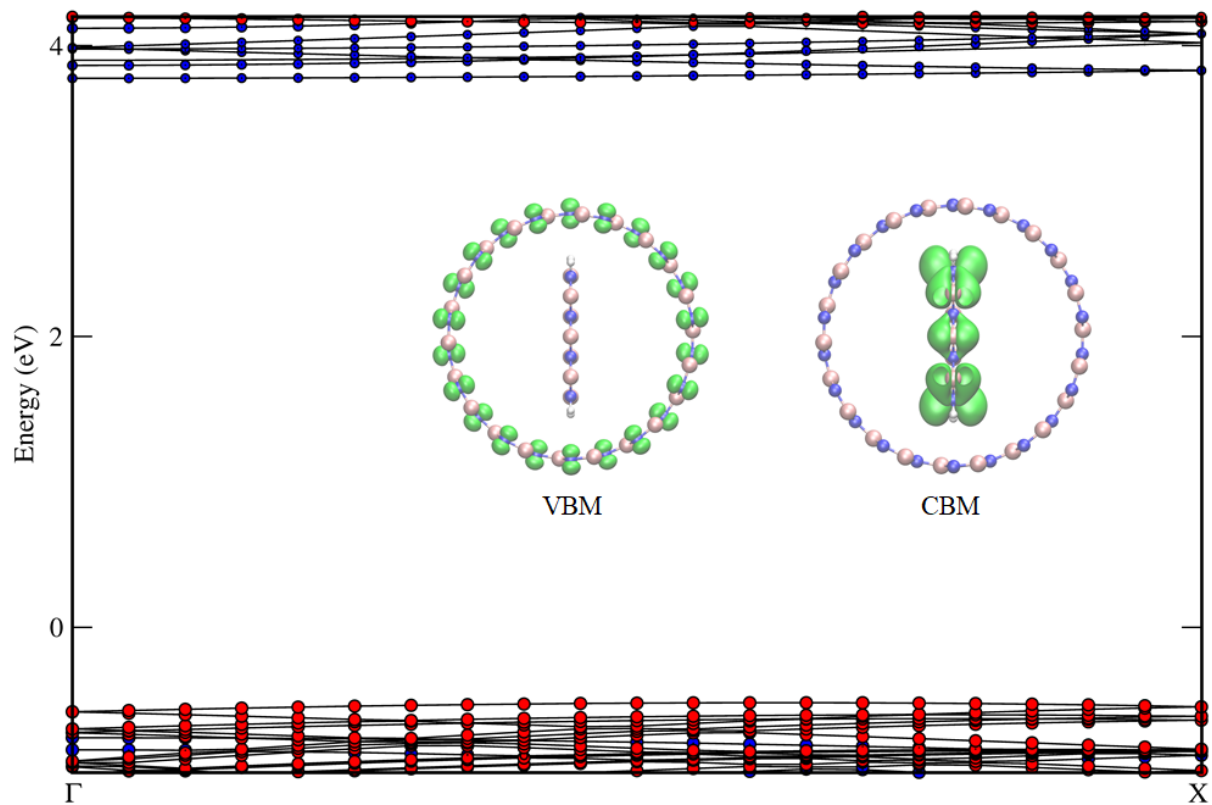


Figure S2 Band structure of BN (11,11)+A₇ (indirect band gap 4.295 eV). The contributions from nanotube and nanoribbon to the energy bands are represented in red and blue spheres, respectively. The charge density distributions of the CBM and the VBM states are shown as inserts (isovalue 0.02 e/Å³).

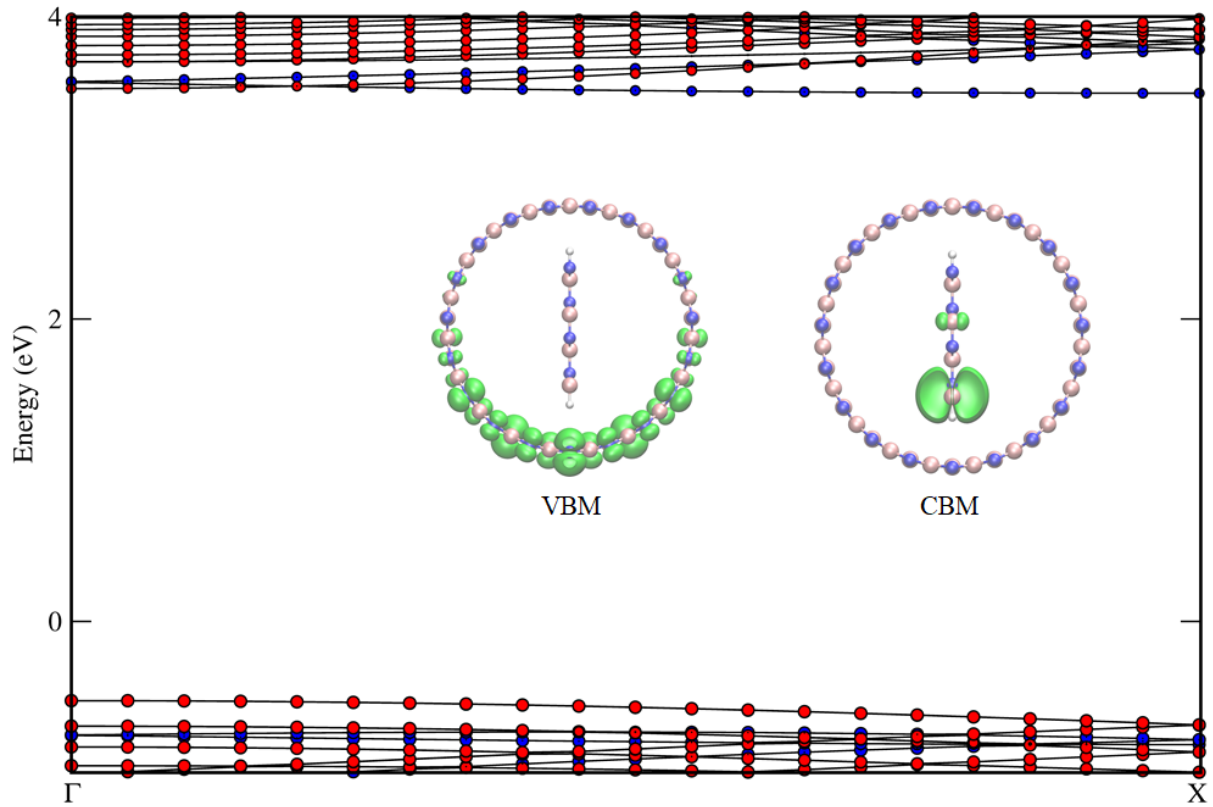


Figure S3 Band structure of BN (19,0)+Z₄ (indirect band gap 4.017 eV). The contributions from nanotube and nanoribbon to the energy bands are represented in red and blue spheres, respectively. The charge density distributions of the CBM and the VBM states are shown as inserts (isovalue 0.02 e/Å³).

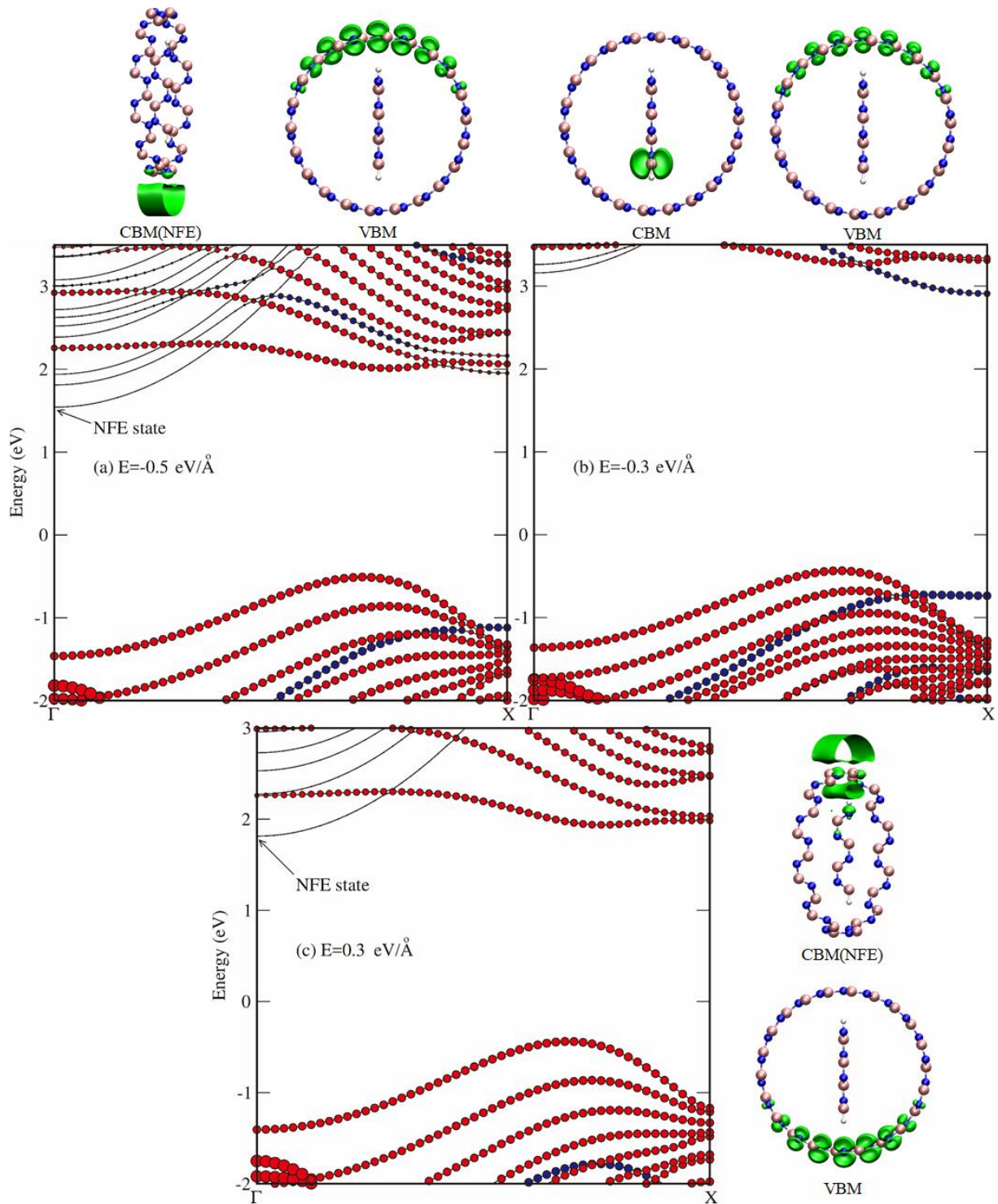


Figure S4 Band structure evolution of (11,11)+Z₄ under electric fields (a) $E=-0.5 \text{ eV/\AA}$ and (b) $E=-0.3 \text{ eV/\AA}$; (c) $E=0.3 \text{ eV/\AA}$. The contributions from NT (NR) to the energy bands are dotted

with red (blue) in the band structure. The evolution of charge density real-space distributions of the CBM and the VBM states are also shown (isovalue $0.012 e/\text{\AA}^3$).

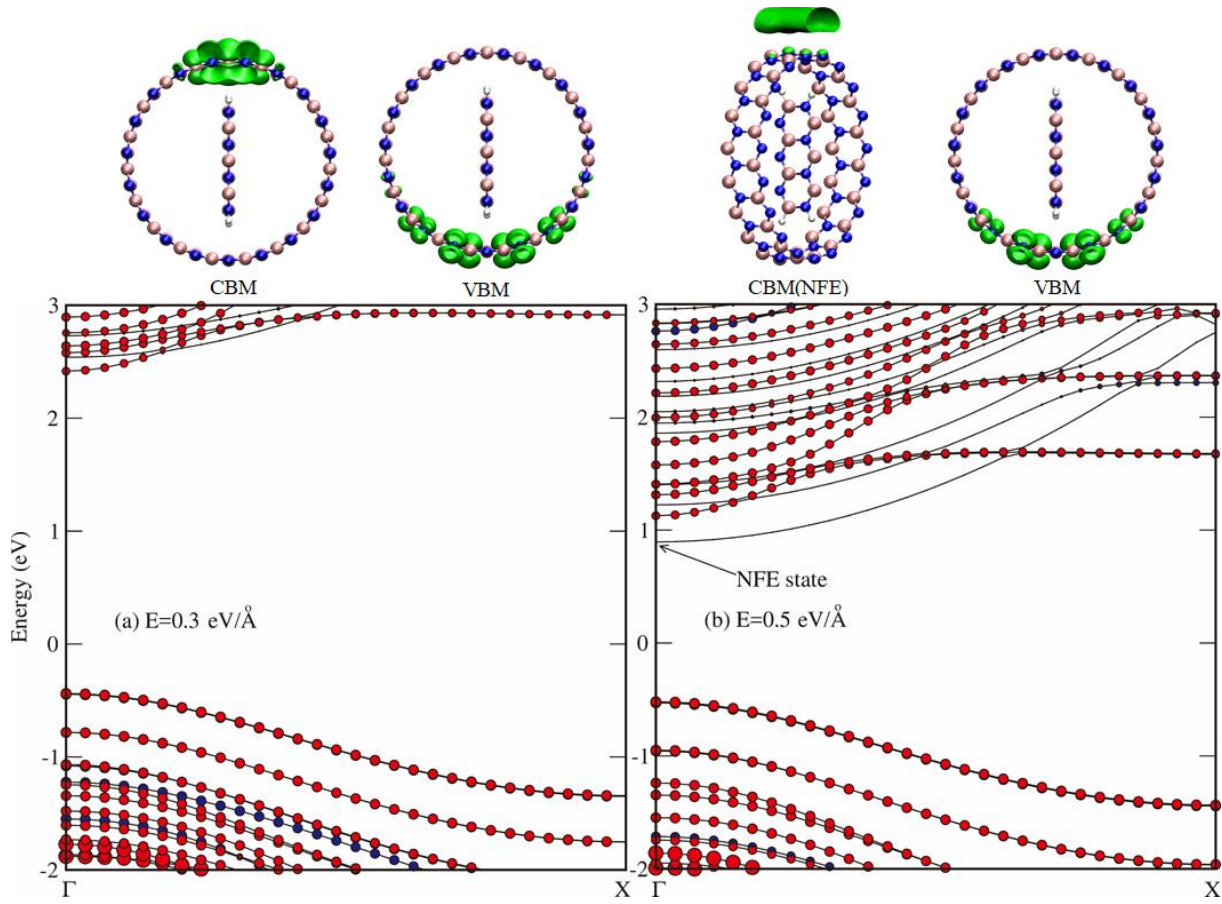


Figure S5 Band structure evolution of $(19,0)+A_7$ under electric fields (a) $E=0.3 eV/\text{\AA}$ and (b) $E=0.5 eV/\text{\AA}$. The contributions from NT (NR) to the energy bands are dotted with red and blue in the band structure. The evolution of charge density real-space distributions of the CBM and the VBM states are also shown (isovalue $0.012 e/\text{\AA}^3$).

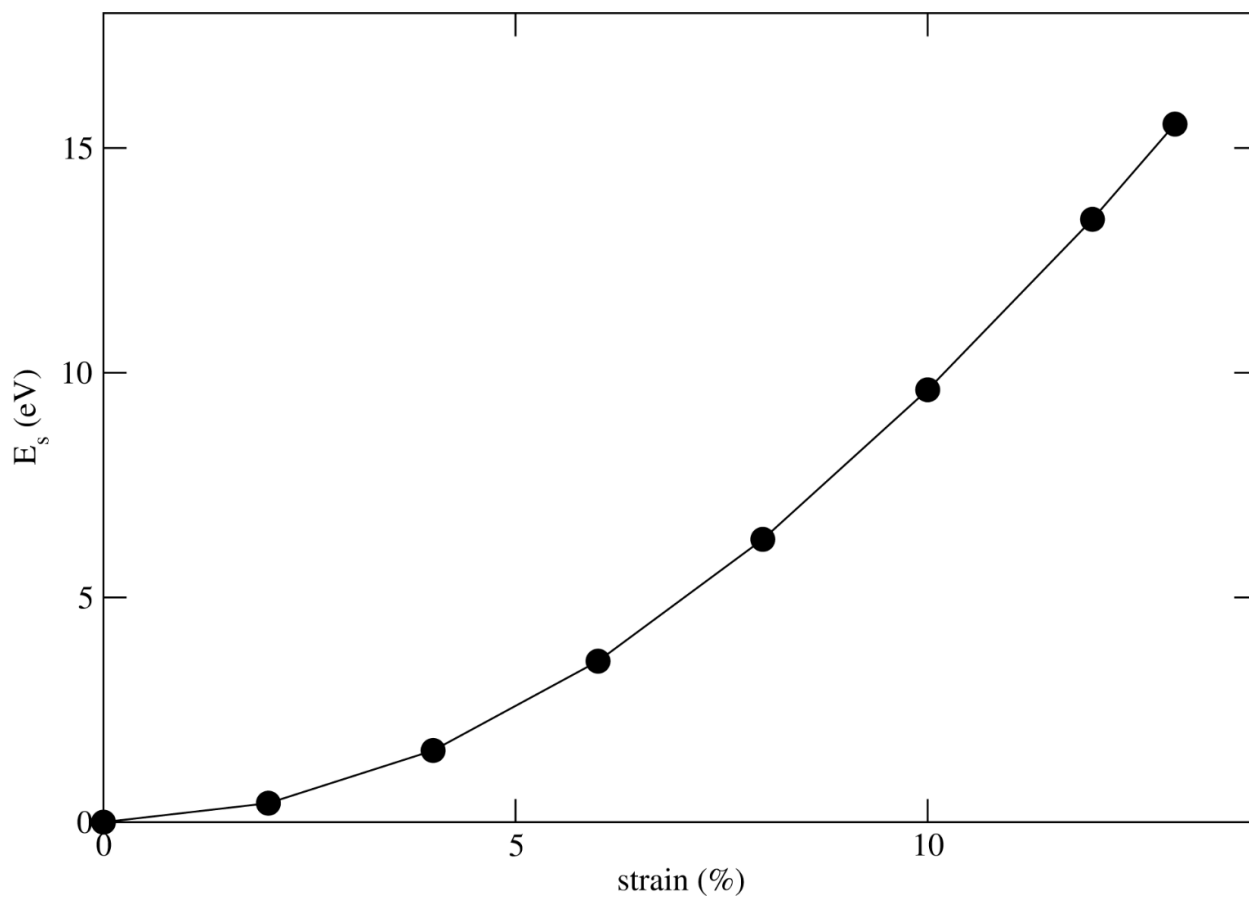


Figure S6 Variation in the total energy of (11,11)+Z₄ with the strain from 0 to 13%.

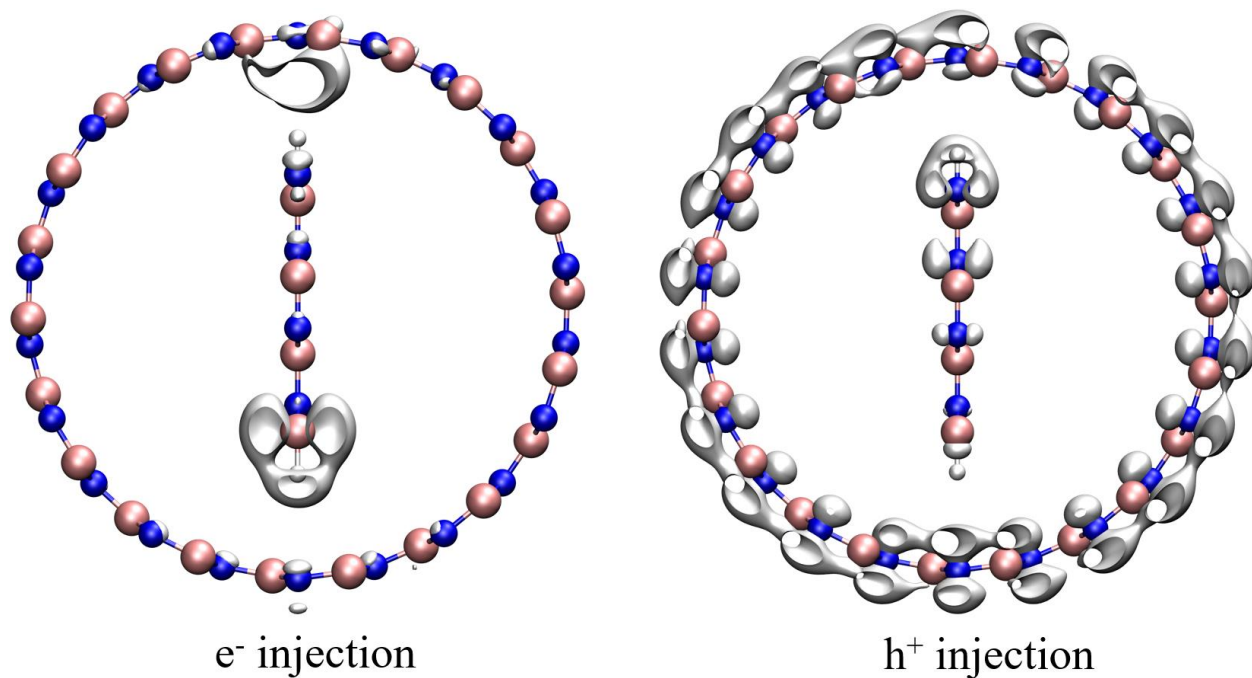


Figure S7 Photo-generated carrier distributions by adding 0.5 extra electron (e^-) or hole (h^+) to each unit of $(11,11)+Z_4$. The isosurface value for e^- or h^+ accumulation is $0.002 e/\text{\AA}^3$.

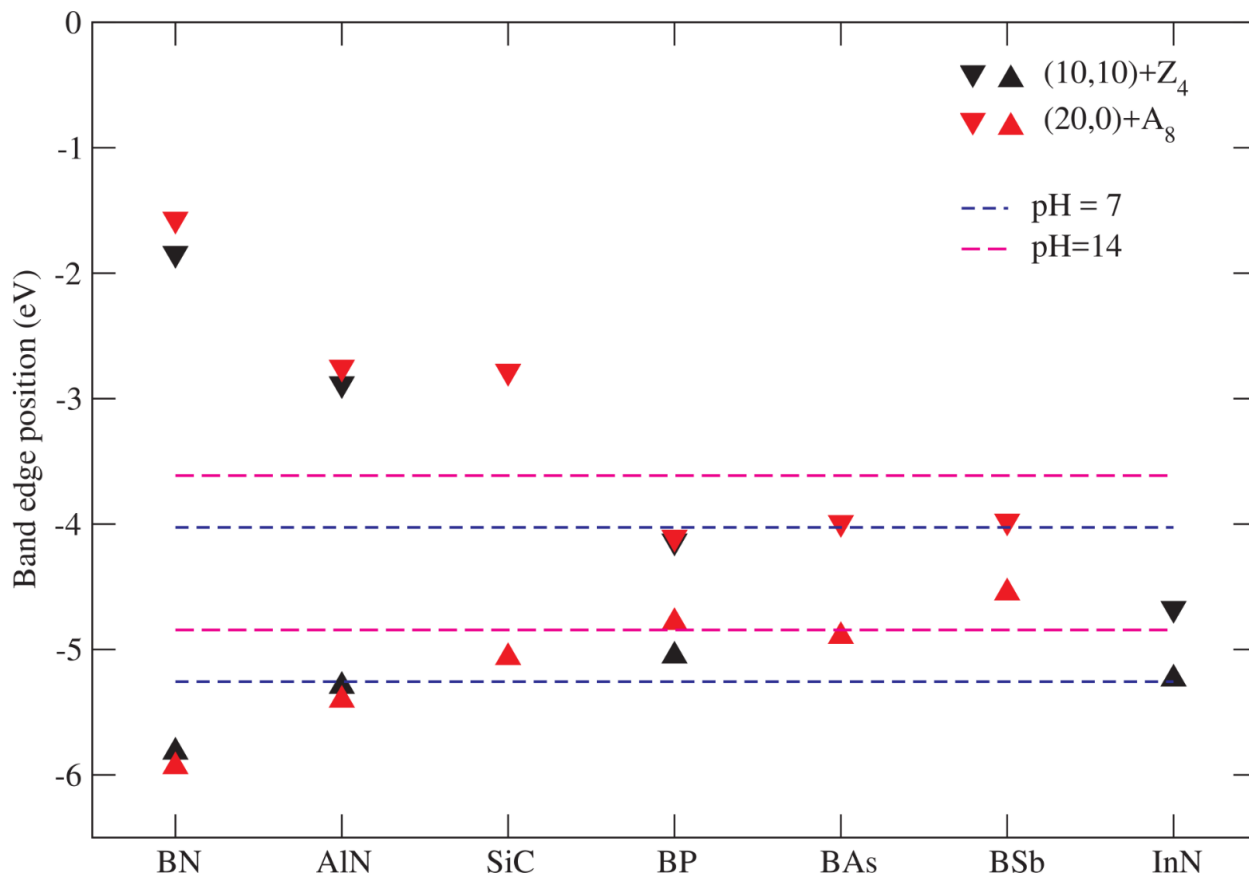


Figure S8 Band alignments relative to the vacuum level for binary group IV-IV and group III-V nanocomposites. The redox potentials of water splitting at pH = 7 (blue dashed lines) and pH = 14 (magenta dashed lines) are shown for comparison.